ISOPHOT Observations of a Cold Filament in the Local Hot Bubble

Uwe Herbstmeier[1] and Alexandre Wennmacher[2]

[1] Max–Planck–Institut für Astronomie, Königstuhl 17, D-69117 Heidelberg, Germany, uherbst@mpia-hd.mpg.de
[2] Institut für Geophysik und Meteorologie der Universität, Albertus-Magnus-Platz, D-50923 Köln, Germany, wennmach@geo.uni-koeln.de

Abstract. We report on FIR measurements of the dust component towards LVC 88+36–2, a dense neutral filament in the Local Hot Bubble. The measurements were performed with ISOPHOT, the photometer on-board ESA's Infrared Space Observatory *ISO* [1]. The dust temperature derived is about 18 K and stays constant across the filament. Limb brightening at 60μm is measured in agreement with cirrus clouds not located in the Local Hot Bubble. No evidence for an increased UV radiation field along the boundaries of the cloud is found.

1 Introduction

Absorption line results towards nearby stars (e.g. Fruscione et al.1994) indicate that the sun's neighbourhood out to about 100 pc is almost void of neutral clouds. Observations with *ROSAT* have demonstrated, however, that several dense clouds are located within this bubble filled with hot gas (Local Hot Bubble, LHB) overlooked by previous measurements. These structures (e.g. Snowden et al.1993, Wang & Yu 1995) cast shadows in the soft X-ray emission of the LHB. The first example for this population was LVC 88+36–2 (Kerp et al.1993), a very elongated gas and dust filament. Sodium absorption lines in the spectra of nearby stars show that the cloud is closer than 60 pc (Wennmacher et al.1992). From HI 21 cm spectral lines Lilienthal & Wennmacher (1990) and Wennmacher (1994) derived an upper limit for the gas temperature of about 150 K and densities up to 100 cm^{-3}.

The cloud-LHB interface is presumably associated with an enhanced local UV radiation field. Conductive boundaries (e.g. Slavin, these proceedings) and/or shock fronts along the edges of the filament (Wennmacher 1994, Draine & McKee 1993) can produce intensities up to an order of magnitude brighter in the EUV than the LISRF. Here, we report on first steps to search for signatures of such a UV field. We present results from far-infrared observations of the dust emission towards LVC 88+36–2 using ISOPHOT

[1] *ISO* is an ESA project with instruments funded by ESA Member States (especially the PI countries: France, Germany, the Netherlands and the United Kingdom) with the participation of ISAS and NASA.

https://doi.org/10.1017/S0252921100070834 Published online by Cambridge University Press

(Lemke et al.1996) on-board ESA's Infrared Space Observatory *ISO* (Kessler et al.1996).

2 Observations and Data Reduction

All measurements with ISOPHOT were performed along a line crossing the filament perpendicularly. Figure 1 shows this line overlayed on the *IRAS* 100 μm image of the filament.

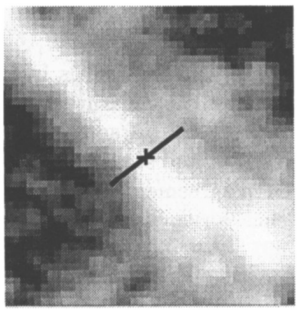

Fig. 1. The *IRAS* 100μm image of LVC 88+36–2 . The line represents the location of the ISOPHOT scans. The reference position, $(\mathrm{RA,DEC})_{\mathrm{J2000}} = (17^{\mathrm{h}}10^{\mathrm{m}}09.4^{\mathrm{s}}, +58°46'30'')$, is marked by a cross. The field extent, oriented along $(\mathrm{RA,DEC})_{\mathrm{J2000}}$, is $1.1° \times 1.1°$.

The FIR measurements were performed at 60, 100, and 170μm using the C100 and C200 detectors. Seven raster points were observed with a step size of 138″ (60 and 100 μm) and 180″ (170 μm). Each scan was performed a second time in opposite direction shifting the line by one pixel width to determine memory effects. The total measurement times per point were 64, 32, and 32 s for 60, 100, and 170μm respectively.

All data were analysed using the ISOPHOT Interactive Analysis PIA[2] V6.1 and associated calibration files. ISOPHOT measurements comprise of integration ramps. These are read-out values of a capacitor voltage integrating the photocurrent of the detector in regular time intervals. The data reduction starts with a correction for non-linearities of this integration process due to the electronics. It includes corrections for glitches on the ramps caused by cosmic ray particle hits. Signals are derived from the slopes of lines fitted to the ramps. A dark signal is subtracted. Transient drifts induced by flux changes were analysed. Only those values were taken for the average signal

[2] PIA is a joint development by the ESA Astrophysics Division and the ISOPHOT Consortium led by the Max-Planck-Institut für Astronomie (MPIA), Heidelberg. Contributing institutes are DIAS, RAL, AIP, MPIK, and MPIA.

https://doi.org/10.1017/S0252921100070834 Published online by Cambridge University Press

per raster point which do not show large signal changes. The signals were calibrated using the associated measurements of one of the Fine Calibration Sources (FCSs), which monitor long-term responsivity drifts. To increase the signal-to-noise ratio the surface brightness values of the pixels were averaged per raster point.

3 Results

In Fig. 2a we plot the resulting surface brightness distributions. The background values derived from the minima were subtracted. The minima were found at a position off the filament towards larger declinations. The brightness peaks are attained at the same raster point with values of 0.42, 1.45, and 3.00 MJy ster^{-1} at 60, 100, and 170μm respectively. The B_{100}/B_{170} brightness ratio there gives a dust temperature of about 18 K assuming a modified (emissivity $\propto \nu^2$) blackbody spectrum.

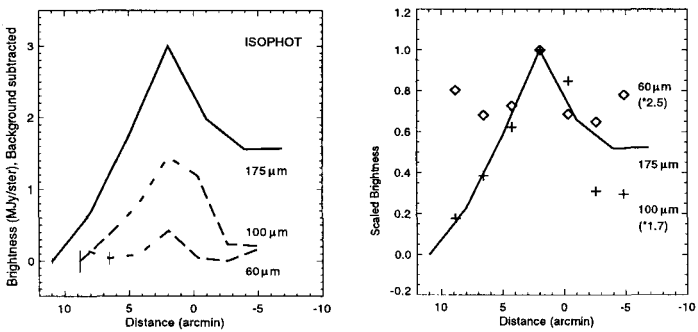

Fig. 2. a) Left: 60, 100, and 170μm surface brightness distribution measured along the scan with respect to the reference position given in Sect. 2, with the same direction as the RA-axis. Typical error bars are indicated by thin lines. **b)** Right: Same as **a)** but for scaled surface brightness. The B_λ/B_{170} ratio at the maximum is taken as the reference ratio. The height of the plotting symbols corresponds to the full width of the error bar.

To look for colour variations across the filament we applied a method developed by Laureijs et al.(1991) similar as in Bogun et al.(1996). The brightness at $\lambda = 60$ and 100μm were scaled with the B_{170}/B_λ ratio derived for the peak. These scaled values were then overplotted on the normalised 170μm scan in Fig. 2b. The distributions should coincide if there were no variations of the infrared colours along the scan. This is the case for the 100μm points towards positive scan offsets. With the exception of one point the B_{100}/B_{170} ratio on the opposite side is lower. The B_{60}/B_{170} ratios are constant in the central part but raise towards both edges.

https://doi.org/10.1017/S0252921100070834 Published online by Cambridge University Press

4 Discussion

Model spectra (e.g. Désert et al.1990) predict that the B_{100}/B_{175} ratio is dominated by the modified blackbody spectrum of the big dust grain component and serves therefore as a good temperature indicator. LVC 88+36–2 is well confined towards larger equatorial coordinates. Here, no variations of the B_{100}/B_{175} ratio (i.e. temperature) are found across the filament edge. On the opposite side the filament merges with a diffuse extended halo. We extract the core's emission from the halo by subtracting a linear brightness gradient as an approximation of the halo. Then the 100/170 colours of the core with the exception of the point at the reference position agree very well with the one derived for the maximum brightness. We like to note without further discussion that the deviating ratio is found at the transition between the core and the halo emission. Also after separation between halo and core emission the B_{60}/B_{175} ratios raise towards the edges of the filament. In addition to the modified blackbody spectrum of the big grains the emission from transiently heated smaller grains contributes to the brightness at 60μm . The constancy of the big grain temperature and the systematic raise of the 60μm brightness indicate variations in the emission characteristics of the small grains. This limb brightening is, however, similarly found for other cirrus clouds not located in the LHB (e.g. Laureijs et al.1991).

Summarising, the ISOPHOT data obtained so far show no evidence for an increased UV radiation field at LVC 88+36–2 . No significant influence of the hot-cold interface or presumed shock fronts along the boundary on the characteristics of the filament's dust component is found.

Acknowledgements. We appreciate discussions with the members of the ISOPHOT Data Centre and the ISOPHOT Instrument Dedicated Team. The ISOPHOT instrument and Data Centre are funded by the Deutsche Agentur für Raumfahrtangelegenheiten DARA and the Max-Planck-Gesellschaft.

References

Bogun S., Lemke D., Klaas U., et al.(1996): A&A 315, L71
Désert F.X., Boulanger F., Puget J.L. (1990): A&A 237, 215
Draine B.T., McKee C.F. (1993): ARA&A 31, 373
Fruscione A., Hawking I., Jelinsky P., & Wiercigroch A. (1994): ApJS 94, 127
Kerp J., Herbstmeier U., & Mebold U. (1993): A&A 268, L21
Kessler M.F., Steinz J.A., Anderegg M.E., et al.(1996): A&A 315, L27
Laureijs R.J., Clark F.O., Prusti T. (1991): ApJ 372, 185
Lemke D., Klaas U., Abolins J., et al (1996): A&A 315, L64
Lilienthal D., & Wennmacher (1990): A&A 235, L13
Snowden S.L., McCammon D., Verter F. (1993): ApJ 409, L21
Wang Q.D., Yu K.C. (1995): AJ 109, 698
Wennmacher A. (1994): PhD Thesis, Universität Bonn
Wennmacher A., Lilienthal D., Herbstmeier U. (1992): A&A 261, L9